



In situ photoelectrocatalytic generation of bactericide for instant inactivation and rapid decomposition of Gram-negative bacteria

Guiying Li^{a,b}, Xiaolu Liu^{a,b}, Haimin Zhang^a, Taicheng An^{a,b,*}, Shanqing Zhang^a, Anthony R. Carroll^a, Huijun Zhao^{a,*}

^a Environment Futures Centre and Griffith School of Environment, Gold Coast Campus, Griffith University, Queensland 4222, Australia

^b State Key Laboratory of Organic Geochemistry, Guangzhou Institute of Geochemistry, Chinese Academy of Sciences, Guangzhou 510640, PR China

ARTICLE INFO

Article history:

Received 16 September 2010

Revised 13 October 2010

Accepted 18 October 2010

Available online 27 November 2010

Keywords:

Bromide

Escherichia coli

Photoelectrocatalytic inactivation

Photoelectrocatalytic decomposition

Mechanisms

ABSTRACT

A bactericidal technique (PEC-Br) utilizing *in situ* photoelectrocatalytically generated photoholes (h^+), long-lived di-bromide radical anions (Br_2^-) and active oxygen species (AOS) for instant inactivation and rapid decomposition of Gram-negative bacteria such as *Escherichia coli* (*E. coli*) was proposed and experimentally validated. The method is capable of inactivating 99.90% and 100% of 9×10^6 CFU/mL *E. coli* within 0.40 s and 1.57 s, respectively. To achieve the same inactivation effect, the proposed method is 358 and 199 times faster than that of the photoelectrocatalytic method in the absence of Br^- , and 2250 and 764 times faster than that of the photocatalytic method in the absence of Br^- . The decomposition experimental results obtained from 600-s PEC-Br-treated samples demonstrated that over 90% of *E. coli* body mass was decomposed and 42% biological carbon contents in the sample was completely mineralized and converted into CO_2 . The mechanistic pathways of disinfection/decomposition by photocatalysis (PC), photoelectrocatalysis (PEC), and photoelectrocatalysis in presence of Br^- (PEC-Br) were also illustrated based on experimental evidence.

© 2010 Elsevier Inc. All rights reserved.

1. Introduction

Advanced oxidation techniques based on TiO_2 photocatalysis have proven to be highly effective for decomposition and mineralization of a wide spectrum of organics [1–5]. Matsunaga and co-workers' pioneering work on sterilizing microbial cells with illuminated TiO_2 particles has opened up a new field of applications for TiO_2 photocatalysis, leading to enormous research opportunities to develop heterogeneous photocatalysis-based bactericidal techniques [6–17]. The main attraction of these bactericidal techniques are the superior oxidative power of photocatalytically generated holes, and the active oxygen species (AOS) including radicals that can readily kill a wide spectrum of waterborne pathogens [6,7,10,12,13,18]. Noticeable progress has been made to demonstrate the bactericidal effects toward a variety of pathogens at illuminated TiO_2 particles in aqueous suspension [7,10,11,18]. Although the lethal killing mechanisms are still under intensive debate, it has been generally accepted that the bactericidal function of TiO_2 photocatalysis can be attributed to the oxidation properties of photocatalytically generated AOS such as

$\cdot OH$, O_2^- , $HOO\cdot$, and H_2O_2 [9,11,12,14,18–21]. In effect, these photocatalytically generated AOS act as bactericides responsible for bacteria death. However, the current bactericidal methods employing photocatalytically generated AOS at TiO_2 normally require 1–6 h of disinfection to achieve total inactivation of a sample with a bacteria population greater than 10^6 colony-forming units/mL (CFU/mL) [9,10,12,20]. This shortcoming in bactericidal efficiency may be attributed to insufficient AOS's *in situ* concentrations that results from the inherent limitations of AOS's short lifetime in aqueous media and rapid recombination with photocatalytically generated electrons [1,22–24]. A new approach is therefore needed in order to overcome these inherent limitations. A possible way to enhance the efficiency of TiO_2 -based bactericidal methods is to utilize the photocatalytic oxidation power of the illuminated TiO_2 to generate different types of bactericidal species with high stability that can sustain high concentrations of bactericidal species. It is well known that halogen radicals are effective bactericides and can be readily produced by photocatalytic oxidation of halide ions at illuminated TiO_2 [25]. The photocatalytic production of high concentration of halogen radicals is possible because these radicals can form stable di-halide radical anions (X_2^-) in the presence of X^- [26,27]. Since the effectiveness of a bactericide is highly dependent on its killing mechanisms [28,29], the bactericidal efficiency may be benefited from the different killing mechanisms offered by halide radicals.

* Corresponding authors. Address: Environment Futures Centre and Griffith School of Environment, Gold Coast Campus, Griffith University, Queensland 4222, Australia. Fax: +86 20 85290706 (T. An), fax: +61 7 5552 8067 (H. Zhao).

E-mail addresses: antc99@gig.ac.cn (T. An), h.zhao@griffith.edu.au (H. Zhao).

Herein, a bactericidal technique utilizing *in situ* photoelectrocatalytically generated photoholes (h^+), Br_2^- , and other AOS to instantly inactivate and rapidly decompose *E. coli* was developed. Moreover, the disinfection and decomposition mechanisms of photocatalysis (PC), photoelectrocatalysis (PEC), and photoelectrocatalysis in the presence of Br^- (PEC- Br) were also illustrated based on experimental evidences.

2. Experimental

2.1. Chemicals and materials

Indium tin oxide conducting glass slides (ITO, 8 Ω /square) were purchased from Delta Technologies Ltd. (USA). Titanium butoxide (97%, Aldrich), chloramine-T (98%, Sigma-Aldrich), nutrient broth and nutrient agar (Oxoid) were used as received. Other chemicals used were of analytical grade and purchased from Aldrich unless otherwise stated. All solutions were prepared using high purity deionized water (Millipore Corp., 18 M Ω cm).

2.2. System setup

Scheme 1 schematically illustrates the experimental system setup. Both photocatalysis and photoelectrocatalysis experiments were performed using the same photoelectrochemical cell that consists of a UV-LED array light source, a TiO₂ photoanode as the working electrode, a Ag/AgCl reference electrode and a Pt mesh auxiliary electrode. The TiO₂ photoanode was prepared by hydrolysis of titanium butoxide according to the method described in our previous work [24]. The thickness of the reaction chamber and the illumination area were 0.25 mm and 462 mm², respectively. The UV-LED array light source consists of four pieces of UV-LED (NCCU033 (T), Nichia Corporation). The specified peak wavelength of the LED was 365 nm with a spectrum half width of 8 nm. The UV intensity was adjusted by a power supply and measured with an UV-irradiance meter (UV-A, Beijing Normal University).

2.3. Bacterial strains, culture conditions, and bacterial cell preparation

As representatives of Gram-negative bacteria, a strain of *E. coli* (K12 derivative strain) was purchased from Southern Biological. The bacterial strain used was inoculated into nutrient broth and grown overnight at 37 °C by constant agitation under aerobic conditions. After incubation, for the suspension system, bacterial cells were harvested by centrifugation at 3000 rpm for 15 min and the bacterial pellet was resuspended in sterile deionized water. This

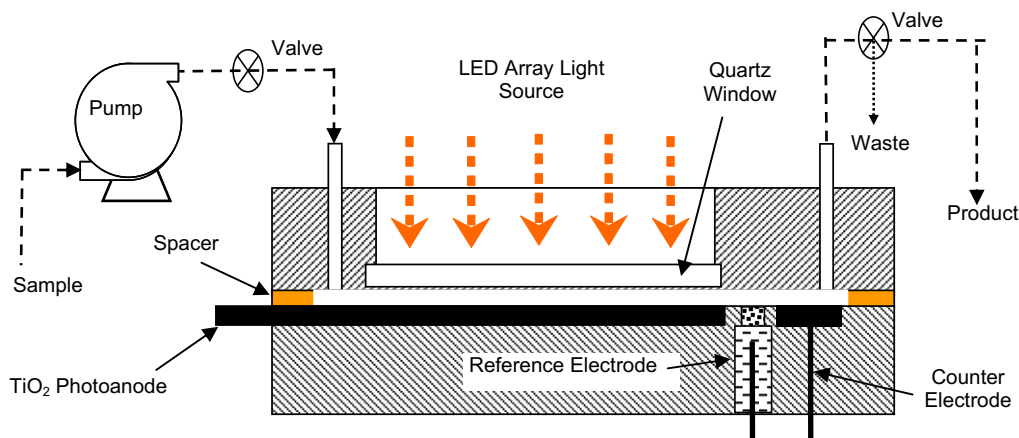
washing step was repeated three times to eliminate residual organic and inorganic substances. Finally, the washed bacterial cells were resuspended in sterile deionized water and were diluted with 0.1 M NaNO₃ solution to obtain suitable concentrations of *E. coli*. For the cell attachment studies, the overnight incubated *E. coli* suspension was used. The cultured bacteria solution was seeded, and fresh nutrient broth was also added in a sterilized petri dish to allow the cell to multiply and attach onto the TiO₂ photoanodes in dark. Subsequently, the enrichment of adhesive microorganisms was conducted in a 37 °C incubator for 72 h in the dark and then the surfaces of the TiO₂ photoanodes were washed by using sterile deionized water to remove reversible attached cells.

2.4. Procedures for inactivation of bacteria

Both PC and PEC disinfection experiments were performed under identical UV intensity using the same UV-LED array photoelectrochemical cell as described in Scheme 1. For the PEC experiments, a 0.1 M NaNO₃ solution was used as the supporting electrolyte. A voltammograph (cv-27, BAS) was used for electrochemical control. Potential and current signals were monitored using a Macintosh computer (7220/200) coupled with a Maclab 400 interface (AD Instruments). A sample containing 9.0×10^6 CFU/mL *E. coli* and 0.1 M NaNO₃ was continuously injected into the cell via a precision pump during the experiment. The reaction time of a sample was controlled by adjusting the flow rate. A sufficient volume of the reacted sample was collected for further analyses after the system reaching its steady-state for which the obtained sample had been subjected to the same reaction time. A 0.1 M NaNO₃ solution was used to clean the cell in between the two sample injections. While for the PEC- Br disinfection experiments, the test solution with an additional 1.0 mM NaBr was employed. PC disinfection experiment was conducted under identical experimental conditions as PEC experiment, except the electrochemical system was disconnected.

2.5. Analysis

E. coli cell viabilities after various disinfection treatments were estimated by means of colony-counting procedure. That is, a collected sample (200 μ L) was spread on nutrient agar plates after serial dilutions (10^{-1} , 10^{-2} , 10^{-3} , 10^{-4} , and 10^{-5}) using the saline solution. After incubating the agar plates for 24 h at 37 °C in the dark, the developed colonies were enumerated and the number of viable cells was recorded in terms of CFU per unit volume of the reaction mixture. It should be noted that the data shown in this



Scheme 1. Schematic diagram of UV-LED photoelectrochemical cell.

work were the average values of data obtained from experiments replicated in triplicate.

The viabilities of *E. coli* were also double confirmed with the BacLight™ kit (Live/Dead BacLight bacterial viability kit, Molecular Probes, Inc.) fluorescent microscopic method. Staining procedure was carried out as proposed by the manufacturer. The fluorescence microscopy observations and picture capture were performed by using a Nikon digital camera (DS-5Mc, Japan) mounted on an Olympus fluorescence microscope (BX51TR, Japan), and the cells in each image was counted to determine the number of cells on the substrates.

Before and after *E. coli* decomposition, the total organic carbon (TOC) contents of samples were examined with TOC – V_{CPH} – V/TOC – V_{CPN} Total Organic Carbon Analyzer (Shimadzu Corporation, Japan). Standardization curves for the inorganic carbon and total carbon determinations were prepared according to the manufacturer's instructions. Triplicate analyses were performed on each sample.

The concentration of Br⁻ before and after PEC–Br treatments was analyzed using standard Phenol Red Colorimetric Method according to the reference [30].

2.6. Sample preparation for scanning electron microscopy (SEM)

Before and after *E. coli* decomposition, the *E. coli* cells attached onto the TiO₂ photoanodes fixed by 3% glutaraldehyde for approximately 60 min at room temperature (or longer in the refrigerator), and then washed with 0.1 M cacodylate buffer (pH 7.4) for 10 min and post fixed for 20 min in 1% osmium tetroxide. Subsequently, the specimens were dehydrated by a graded series of ethanol (70%, 90%, and 100%) and 100% amyl acetate two times each for 10 min, respectively. The cells on the substrates were finally critical point dried by using Denton Vacuum critical point dryer (Denton Vacuum, Inc., USA), gold sputter coated on the substrates and were visualized using a scanning electron microscope (JEOL JSM-6300F).

3. Results and discussion

3.1. Inactivation of *E. coli* by PC, PEC and PEC–Br methods

The samples containing 9.0×10^6 CFU/mL *E. coli* were subjected to inactivation treatment by PEC–Br, PEC, and PC methods under comparable experimental conditions (see Fig. 1). For PEC–Br experiments, the sample solutions containing 9.0×10^6 CFU/mL *E. coli*,

0.10 M NaNO₃, and 1.0 mM Br⁻ were used. The photoelectrocatalysis was performed under a +0.30 V (vs. Ag/AgCl) applied potential bias. Fig. 1a shows the number of surviving *E. coli* plotted against *E. coli* resident time (disinfection time), obtained from PEC–Br-treated samples. It reveals that 99.90% of *E. coli* can be inactivated within 0.40 s while 100% inactivation occurs by 1.57 s. This demonstrates a near instantaneous inactivation capability for the PEC–Br method. For comparison, PEC (Fig. 1b) and PC (Fig. 1c) inactivation experiments in the absence of Br⁻ were performed under identical experimental conditions as PEC–Br experiments. It can be seen from Fig. 1b that the number of survived *E. coli* with the PEC-treated samples gradually decreased as the resident time increased. It took 143 s to achieve 99.90% inactivation and a further 169 s to achieve 100% inactivation. This means that to achieve the same inactivation effect, the PEC method is 358 (99.90% inactivation) and 199 times (100% inactivation) slower than that of the PEC–Br method. For the PC-treated samples, 900 s and 1200 s were needed to achieve 99.92% and 99.99% inactivation (Fig. 1c). These intervals are 2250 and 764 times larger than that of the PEC–Br treatment. It should be noted that the data shown in Fig. 1 were the average values of data obtained from experiments replicated in triplicate. The bacterial viability of all experiments was determined using standard plate count method to assess the treated samples after 24-h incubation at 37 °C. All reported data were double confirmed with the BacLight™ kit fluorescent microscopic method. Fig. 2 shows the typical fluorescent microscopic images of viable cells of an *E. coli* sample before treatment and after 0.40 s and 1.57 s of PEC–Br treatment. The viable cells only accumulate rhodamine 123, appearing as 'green' under fluorescent microscope, while dead cells having damaged cytoplasmic membranes accumulate both rhodamine 123 and propidium iodide that are expressed as 'red' in the fluorescent microscopic image [31]. The bactericidal effects shown in Fig. 1 demonstrate that the presence of Br⁻ shortens the required inactivation time by 2–3 orders of magnitude. Although the PEC–Br, PEC, and PC systems are all capable of *in situ* generating AOS as bactericides, it is clear that the bactericides produced in the presence of Br⁻ are responsible for the dramatically enhanced bactericidal effect. The mechanistic aspects of the enhancement are consequently investigated.

3.2. Decomposition of *E. coli* by PC, PEC, and PEC–Br methods

Field-Emission Scanning Electron Microscopy (FESEM) was employed to examine the location and extent damages to *E. coli* cells attached to the TiO₂ substrate after PC, PEC, and PEC–Br treatments. The untreated *E. coli* cell (Fig. 3a) exhibits well-preserved cell walls. FESEM examination reveals no obvious damage when the sample was subjected to a short period of PC treatment (i.e., 60 s). However, a 900-s PC treatment leads to severe damages to the cell membrane (Fig. 3b). These damages occurred mainly on the cell body parts that were in direct contact or close to the TiO₂ surface where the concentrations of AOS are relatively high. Damages to other parts of the cell body were also observed. Considering the short lifetime of oxygen radicals such as 'OH and HOO', more stable AOS such as H₂O₂ are likely to be responsible for damages at these locations, as illustrated in Scheme 2a and b. Fig. 3c shows FESEM image of an *E. coli* cell after 60 s of PEC treatment. The PEC-treated cells were found to be flattened on the TiO₂ photoanode surface due to the excessive damage to the cell body that was in direct contact with the photoanode surface. In contrast to the PC-treated cells, no obvious damages to the cell body that was not in direct contact with the photoanode surface was observed, suggesting the domination of direct photohole reactions in a PEC system. Unlike a PC process, a PEC process employs a potential bias (i.e., +0.30 V vs. Ag/AgCl) as an external driving force to timely remove the photoelectrons from TiO₂ conduction band to

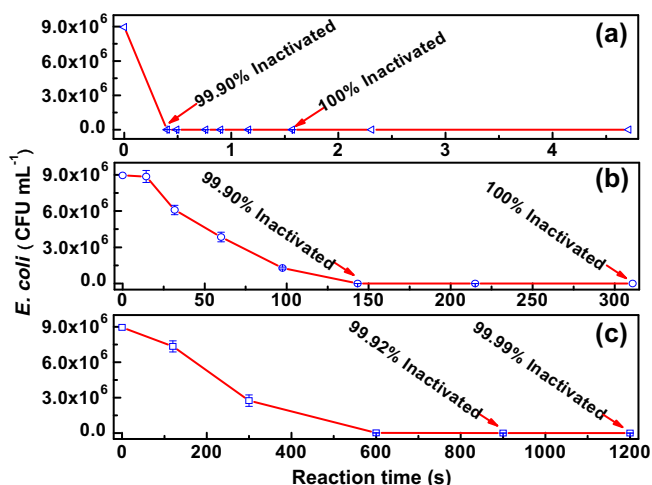


Fig. 1. Survived *E. coli* plot against resident time for (a) PEC–Br-treated, (b) PEC-treated, and (c) PC-treated samples.

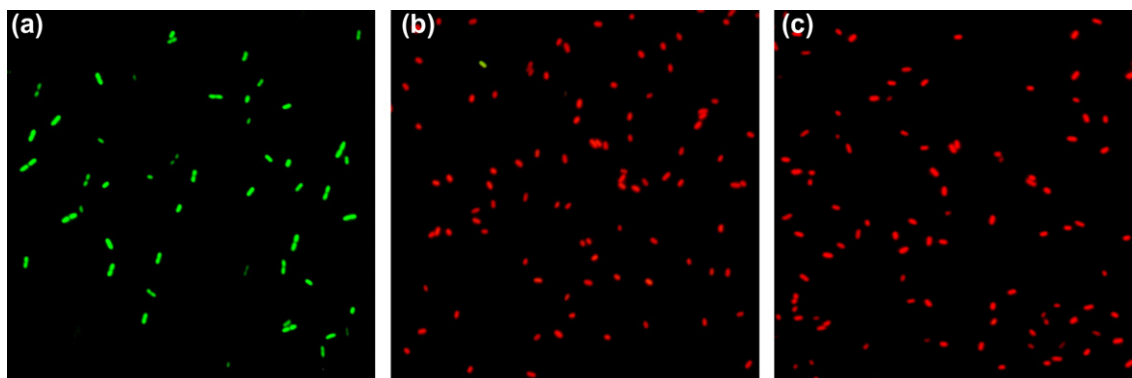


Fig. 2. Fluorescent microscope images of *E. coli* (a) without treatment; (b) after 0.40 s; and (c) 1.57 s of PEC-Br treatment.

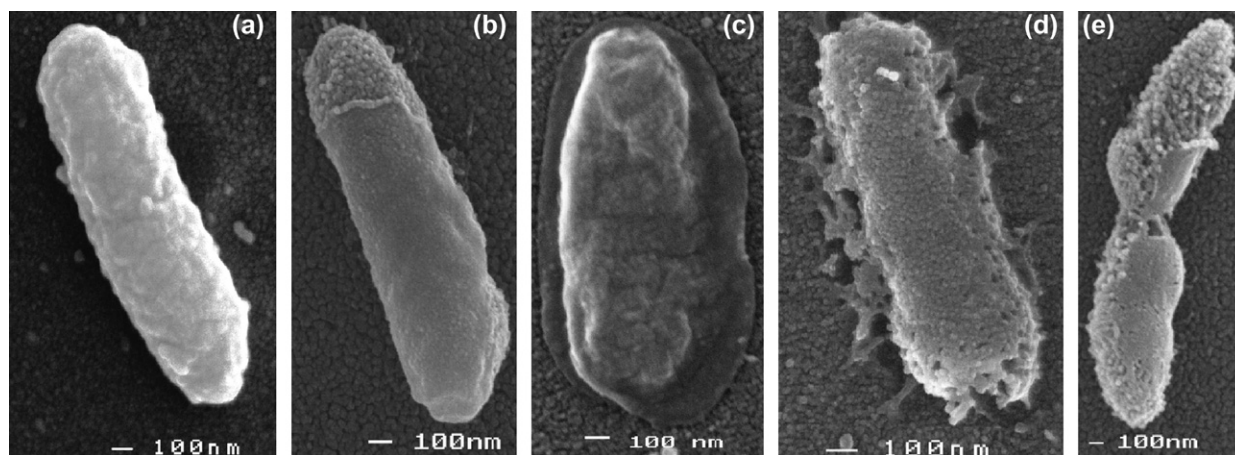
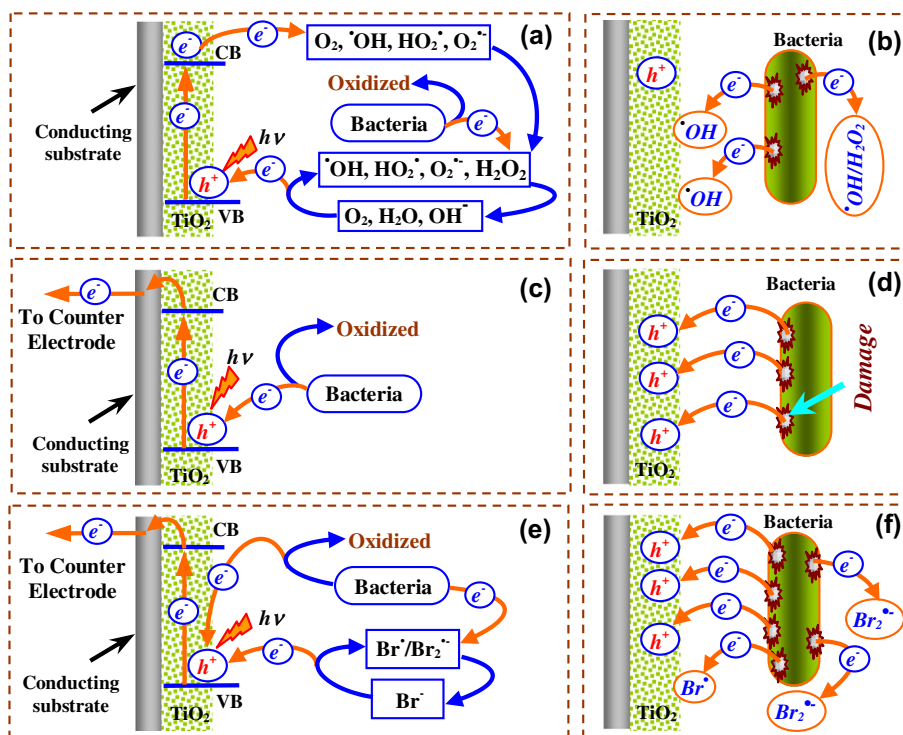


Fig. 3. FESEM images of *E. coli* cell attached to the TiO_2 photoanode. (a) without treatment; (b) after 900 s of PC treatment; (c) after 60 s of PEC treatment; (d) after 300 s of PEC treatment; and (e) after 60 s of PEC-Br treatment.



Scheme 2. Decomposition mechanisms of *E. coli* by (a and b) PC treatment; (c and d) PEC treatment; (e and f) PEC-Br treatment.

the external circuit then to the counter electrode where the electrons are consumed by forced reduction reactions [1,22–24]. As a result, the recombination reactions are effectively suppressed, leading to enhanced photocatalytic efficiency [1,22–24,32]. The ability of a PEC process to timely remove photoelectrons and physically separate the reduction half-reactions (at counter electrode) from the oxidation half-reactions (at TiO₂ photoanode) prolongs the lifetime of photoholes [2], enabling the photohole to directly act as the bactericide to react with bacteria. The strong oxidative power of the photohole (+3.1 V) could rapidly damage/decompose the cell body that is in direct contact to the photoanode surface, as illustrated in Scheme 2c and d. It must be noted that in a PEC process, photocatalytic generation of AOS still occur and with an even higher intensity due to the suppressed recombination reactions. The observed damages from Fig. 3c are the collective effect of AOS and the direct photohole reactions. There are no visible damages to cell bodies that are not in direct contact with the photoanode surface, because the photoholes only exist within the TiO₂ (Scheme 2d), and AOS could not cause visible damage within 60 s reaction time. Damages caused by AOS can be clearly evidenced by the FESEM image obtained from a 300-s PEC-treated sample for which decomposition of whole cell body is observed (Fig. 3d). In terms of locations and severity, the observed damages from a 60-s PEC–Br-treated cell differ remarkably from those observed for PEC-treated cell (Fig. 3e). These damages occurred over almost the entire cell body rather than just at the contact between the cell body and the photoanode. The severity of the observed damages is more extensive as evidenced by the significantly decomposed cell body. In fact, the cell body could be completely decomposed with an extended reaction time. Fig. 4 shows FESEM images of cells after 120 s, 300 s, and 600 s of PEC–Br treatment, respectively. These images represent typical damages of majority cells under the given experimental conditions. For majority cells, over 90% of their body mass was decomposed after 600-s PEC–Br treatment (Fig. 4c). It should be noted that all SEM images shown in this work are typical images and representative for the specified experimental conditions. The decomposition products were examined by TOC and HPLC–MS. The extent of mineralization was quantified by TOC decrease during the PEC–Br treatment process (see Fig. 5). A 42% decrease in TOC was observed for a 600-s PEC–Br-treated sample, suggesting nearly half biological carbon contents in a cell were completely mineralized and converted into CO₂. The decomposition products of the incomplete-mineralized components are highly complex. HPLC–MS analysis reveals that the incomplete-mineralized components consist of a wide spectrum of compounds ranging from large organic/biological species to small biological compounds (i.e., amino acids) and simple organic compounds (i.e., formic acid). These results demonstrate a superior

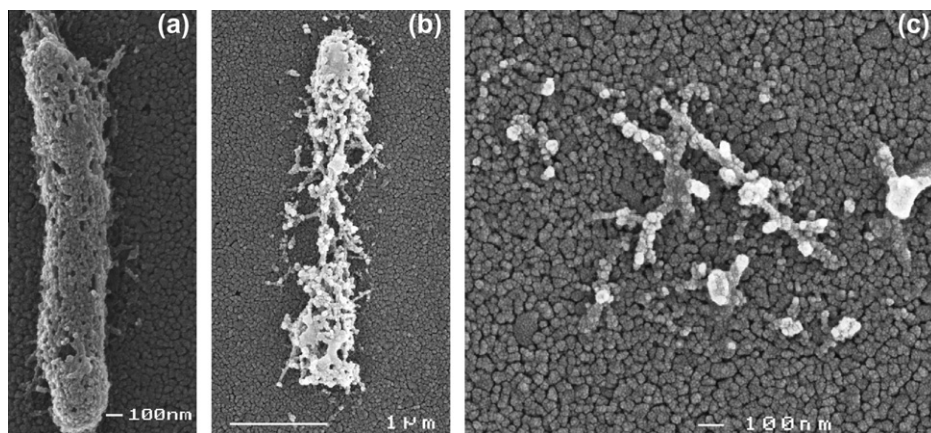


Fig. 4. FESEM images of *E. coli* cell attached to the TiO₂ photoanode after: (a) 120 s; (b) 300 s; (c) 600 s of PEC–Br treatment.

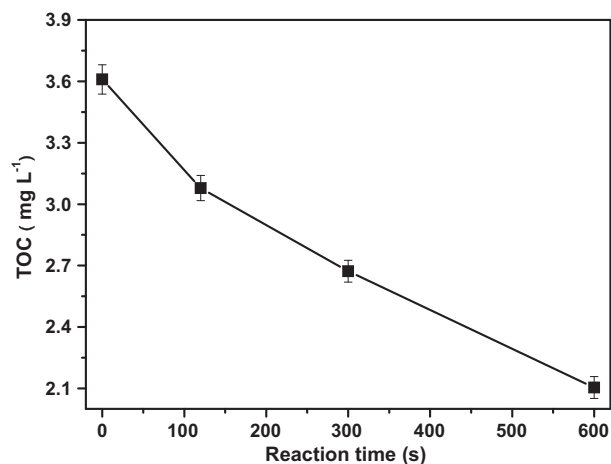
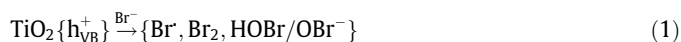


Fig. 5. TOC removal during PEC–Br treatment of *E. coli*.

performance of PEC–Br treatment. Considering that except the addition of 1.0 mM NaBr for PEC–Br treatment, all other experimental conditions employed are identical for both PEC and PEC–Br treatments, it is reasonable to assume that the dramatic performance enhancement observed from PEC–Br treatment is due to the presence of Br⁻, as illustrated in Scheme 2e and f. Hence, the mechanistic role of Br⁻ is investigated.

3.3. Mechanistic considerations

Photoelectrocatalytic oxidation of Br⁻ was performed (see Fig. 6). As the photocurrent obtained in the absence of Br⁻ (0.10 M NaNO₃) is originated from photocatalytic oxidation water, thus the magnitude of the photocurrent is directly proportional to the rate of AOS production [1,24]. An increase in Br⁻ concentration leads to an increase in the photocurrent. The net photocurrent increase is directly proportional to the rate of Br⁻ oxidation. The full spectrum of Br⁻ oxidation pathways is complex because Br⁻ can be oxidized to a variety of oxidation states (e.g., Br₂[0], BrO⁻[+1], BrO₂⁻[+3], BrO₃⁻[+5], or BrO₄⁻[+7]) [33–35]. However, to serve the needs of the present work, the Br⁻ photocatalytic oxidation processes can be simplified and presented as:



The species shown in Eq. (1) are the possible bromide photocatalytic oxidation products [25]. Considering the relatively low standard potentials of Br₂/Br⁻ and HOBr/Br⁻ (+1.087 V and +1.33 V,

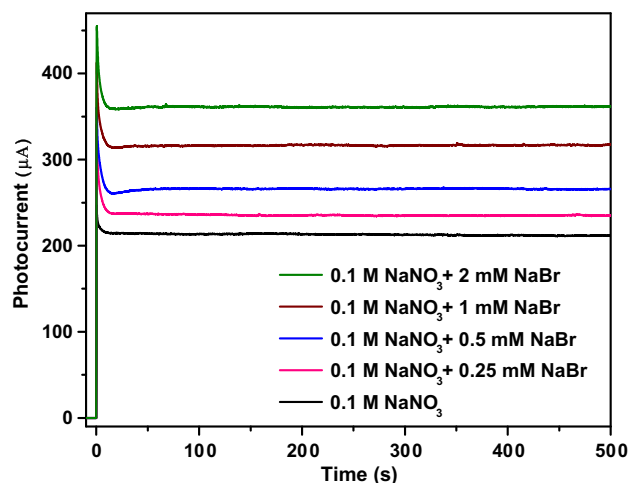
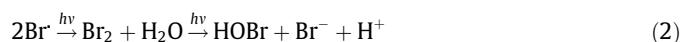
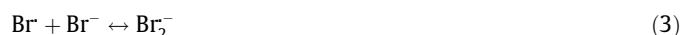


Fig. 6. Photocurrent–time profiles obtained from solutions containing 0.10 M NaNO₃ and different concentrations of NaBr under a typical light intensity of 8.0 mW/cm² (measured at 365 nm) and applied potential bias of +0.30 V vs. Ag/AgCl.

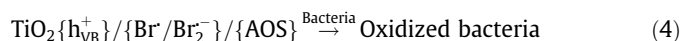
respectively), it is unlikely that these active bromines are responsible for the instant inactivation and rapid decomposition of bacteria. To confirm this, *E. coli* samples used for PEC–Br experiments were treated for 10 s with 1 mM of Br₂ in the absence of TiO₂. The treatment achieved only 2% *E. coli* inactivation and no visible decomposition was observed. This implies that Br₂ and HOBr are not the dominant bactericides in PEC–Br process. Among all species shown in Eq. (1), only Br[•] is directly produced by photocatalysis as the Br₂ and HOBr are produced from photocatalytically generated Br[•] via the following pathways:



This means that the net photocurrent increase shown in Fig. 6 represents the increased rate of Br[•] production and *in situ* photoelectrocatalytically produced Br[•] is the dominant bactericide (Scheme 2e). The superior bactericidal performance of Br[•] can be attributed to its highly reactive nature, strong oxidation power ($E^0[\text{Br}^{\bullet}/\text{Br}^-] = +1.96 \text{ V}$) [27] and the ability to form stable di-bromide radical anions (Eq. (3)) [26].



The formation of Br₂^{•-} prolongs the lifetime of Br[•] to maximize the bactericidal effect. The formation of Br₂^{•-} also enables Br[•] surviving the solution process to cause damages on cell body parts that are not in direct contact with the photoanode (Scheme 2f). It must note that the PEC–Br process retains all advantageous attributes of a PEC process. That is, the photoelectrocatalytically generated AOS and direct photohole reactions are also important attributes. Therefore, the overall bactericidal performance for PEC–Br method should be presented as:



For photocatalysis, the exact lethal killing mechanisms are still unclear [6,14,20]. Nevertheless, we are reasonably confident that for PEC–Br process, the instant damages to the outer cell membrane by the direct photohole reactions are responsible for the cell death. Fig. 7 shows a typical FESEM image of a 2-s PEC–Br-treated *E. coli* cell. The outer membrane of such an inactivated cell remains intact but shape of the cell is buckled, caused by the direct photohole damages to the cell membrane in direct contact with the photoanode. The observed vesicles released from the outer membrane during the cell death process indicate a typical Gram-negative bacterial

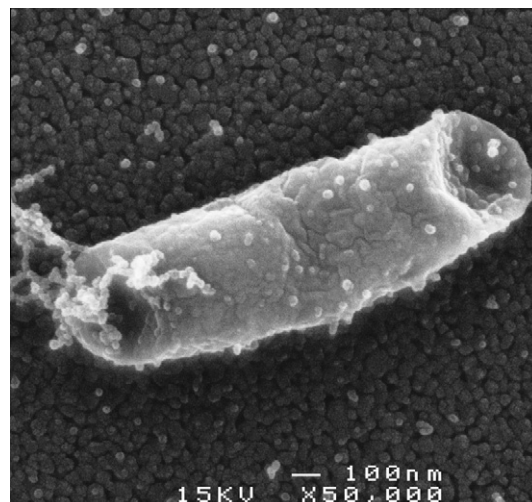
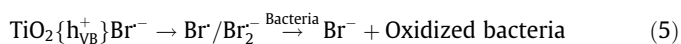


Fig. 7. FESEM image of *E. coli* cell attached to the TiO₂ photoanode after 2 s of PEC–Br treatment.

defense response to stresses caused by external stimulations (i.e., direct photohole oxidation of outer membrane) [36,37].

The concentration of Br⁻ before and after 60 s, 300 s, and 600 s of PEC–Br treatments was analyzed using standard Phenol Red Colorimetric Method to further explore the mechanistic role of Br⁻. For all cases investigated, no essential Br⁻ concentration changes were observed, which agrees with previous observations [33,38]. This suggests that in a PEC–Br process, Br⁻ acts as an “electron mediator”. It is firstly photoelectrocatalytically oxidized to Br[•] and regenerated when Br[•] is reduced by bacteria or other organics:



It should be noted that the bactericidal performance of other halides was also investigated. F⁻ is stable at the illuminated TiO₂ surface as it requires higher oxidation power to oxidize it ($E^0[\text{F}^{\bullet}/\text{F}^-] = +3.6 \text{ V}$) [3]. No noticeable bactericidal effect was observed with I⁻ due to the insufficient oxidation power of I[•] ($E^0[\text{I}^{\bullet}/\text{I}^-] = +1.33 \text{ V}$) [39]. A noticeable bactericidal effect of Cl⁻ was observed, but it was much less effective when compared to Br⁻. The PEC–Cl treatment requires at least 20 times longer disinfection time than that of PEC–Br to achieve the same inactivation effects. Thermodynamically, Cl[•] should be a more effective bactericide due to its high oxidation potential ($E^0[\text{Cl}^{\bullet}/\text{Cl}^-] = +2.41 \text{ V}$) [39]. The lower effectiveness of PEC–Cl treatment may be attributed to the slower Cl₂^{•-} formation kinetics and inferior stability of formed Cl₂^{•-} [40].

4. Conclusions

The notable features of the photoelectrocatalytic bactericidal method investigated here are the mechanisms of *in situ* generating effective bactericides and their ability to instantaneously inactivate and rapidly decompose Gram-negative bacteria such as *E. coli*. The photoelectrocatalysis combines electrochemistry with photocatalysis to effectively suppress the recombination of photoelectrons and holes, prolongs the lifetime of photoholes to enable instantaneous inactivation via direct photohole reactions, and produces higher concentrations of Br[•]/Br₂^{•-} and AOS to achieve rapid decomposition. In theory, the proposed method can be used to *in situ* generate different bactericides that are effective for viruses and other types of bacteria. It could also be applied to decompose organic pollutants.

Acknowledgments

Authors thank Dr. Deborah Stenzel for her help on SEM sample preparations, and Australian Research Council, NSFC (No. 21077104) and Chinese Scholarship Council for financial support.

References

- [1] H.J. Zhao, D.L. Jiang, S.Q. Zhang, W. Wen, *J. Catal.* 250 (2007) 102–109.
- [2] D.L. Jiang, S.Q. Zhang, H.J. Zhao, *Environ. Sci. Technol.* 41 (2007) 303–308.
- [3] K. Lv, Y.M. Xu, *J. Phys. Chem. B* 110 (2006) 6204–6212.
- [4] J.T. Carneiro, J.A. Moulijn, G. Mul, *J. Catal.* 273 (2010) 199–210.
- [5] T.C. An, H. Yang, G.Y. Li, W.H. Song, W.J. Cooper, X.P. Nie, *Appl. Catal. B: Environ.* 94 (2010) 288–294.
- [6] T. Matsunaga, R. Tomoda, T. Nakajima, H. Wake, *FEMS Microbiol. Lett.* 29 (1985) 211–214.
- [7] T.H. Bui, C. Felix, S. Pigeot-Remy, J.M. Herrmann, P. Lejeune, C. Guillard, *J. Adv. Oxid. Technol.* 11 (2008) 510–518.
- [8] D.S. Kim, S.Y. Kwak, *Environ. Sci. Technol.* 43 (2009) 148–151.
- [9] Z.X. Lu, L. Zhou, Z.L. Zhang, W.L. Shi, Z.X. Xie, H.Y. Xie, D.W. Pang, *P. Shen, Langmuir* 19 (2003) 8765–8768.
- [10] A.K. Benabbou, Z. Derriche, C. Felix, P. Lejeune, C. Guillard, *Appl. Catal. B: Environ.* 76 (2007) 257–263.
- [11] M.R. Elahifard, S. Rahimnejad, S. Haghghi, M.R. Gholami, *J. Am. Chem. Soc.* 129 (2007) 9552–9553.
- [12] D.M. Blake, P.C. Maness, Z. Huang, E.J. Wolfrum, J. Huang, W.A. Jacoby, *Separ. Purif. Methods* 28 (1999) 1–50.
- [13] P.S.M. Dunlop, T.A. McMurray, J.W.J. Hamilton, J.A. Byrne, *J. Photoch. Photobio. A* 196 (2008) 113–119.
- [14] T. Matsunaga, R. Tomoda, T. Nakajima, N. Nakamura, T. Komine, *Appl. Environ. Microbiol.* 54 (1988) 1330–1333.
- [15] O.K. Dalrymple, E. Stefanakos, M.A. Trotz, D.Y. Goswami, *Appl. Catal. B: Environ.* 98 (2010) 27–38.
- [16] D.Q. Zhang, G.S. Li, J.C. Yu, *J. Mater. Chem.* 20 (2010) 4529–4536.
- [17] A.G. Rincon, C. Pulgarin, *Catal. Today* 124 (2007) 204–214.
- [18] M. Cho, H. Chung, W. Choi, J. Yoon, *Water Res.* 38 (2004) 1069–1077.
- [19] K. Sunada, T. Watanabe, K. Hashimoto, *Environ. Sci. Technol.* 37 (2003) 4785–4789.
- [20] H. Zheng, P.C. Maness, D.M. Blake, E.J. Wolfrum, S.L. Smolinski, W.A. Jacoby, *J. Photoch. Photobio. A* 130 (2000) 163–170.
- [21] P.C. Maness, S. Smolinski, D.M. Blake, Z. Huang, E.J. Wolfrum, W.A. Jacoby, *Appl. Environ. Microbiol.* 65 (1999) 4094–4098.
- [22] P.A. Mandelbaum, A.E. Regazzoni, M.A. Blesa, S.A. Biles, *J. Phys. Chem. B* 103 (1999) 5505–5511.
- [23] D.L. Jiang, H.J. Zhao, S.Q. Zhang, R. John, *J. Phys. Chem. B* 107 (2003) 12774–12780.
- [24] H.J. Zhao, D.L. Jiang, S.Q. Zhang, K. Catterall, R. John, *Anal. Chem.* 76 (2004) 155–160.
- [25] H. Selcuk, H.Z. Sarikaya, M. Bekbolet, M.A. Anderson, *Chemosphere* 62 (2006) 715–721.
- [26] M.M. Cheng, A. Bakac, *J. Am. Chem. Soc.* 130 (2008) 5600–5605.
- [27] G. Merenyi, J. Lind, *J. Am. Chem. Soc.* 116 (1994) 7872–7876.
- [28] M.A. Kohanski, D.J. Dwyer, B. Hayete, C.A. Lawrence, J.J. Collins, *Cell* 130 (2007) 797–810.
- [29] A.A. Belaouaj, K.S. Kim, S.D. Shapiro, *Science* 289 (2000) 1185–1187.
- [30] APHA, AWWA, WEF, *Standard Methods for the Examination of Water and Wastewater*, Washington, DC, 1995.
- [31] G. Nebe-von-Caron, P.J. Stephens, C.J. Hewitt, J.R. Powell, R.A. Badley, *J. Microbiol. Methods* 42 (2000) 97–114.
- [32] K. Vinodgopal, S. Hotchandani, P.V. Kamat, *J. Phys. Chem. – US* 97 (1993) 9040–9044.
- [33] L.A.T. Espinoza, F.H. Frimmel, *Water Res.* 42 (2008) 1778–1784.
- [34] H. Noguchi, A. Nakajima, T. Watanabe, K. Hashimoto, *Water Sci. Technol.* 46 (2002) 27–31.
- [35] H. Noguchi, A. Nakajima, T. Watanabe, K. Hashimoto, *Environ. Sci. Technol.* 37 (2003) 153–157.
- [36] P. Amezaga-Madrid, R. Silveyra-Morales, L. Cordoba-Fierro, G.V. Nevarez-Moorillon, M. Miki-Yoshida, E. Orrantia-Borunda, F.J. Solis, *J. Photoch. Photobio. B* 70 (2003) 45–50.
- [37] A.J. McBroom, M.J. Kuehn, *Mol. Microbiol.* 63 (2007) 545–558.
- [38] J.M. Herrmann, P. Pichat, *J. Chem. Soc. Farad. Trans. 1* 76 (1980) 1138–1146.
- [39] J.E. Rogers, B. Abraham, A. Rostkowski, L.A. Kelly, *Photochem. Photobiol.* 74 (2001) 521–531.
- [40] Y. Liu, A.S. Pimentel, Y. Antoku, B.J. Giles, J.R. Barker, *J. Phys. Chem. A* 106 (2002) 11075–11082.